HHS Public Access

Author manuscript

J Pathol. Author manuscript; available in PMC 2021 March 31.

Published in final edited form as:

J Pathol. 2020 July ; 251(3): 336–347. doi:10.1002/path.5469.

Trop2 is Upregulated in the Transition to Dysplasia in the Metaplastic Gastric Mucosa

Katherine M. Riera[2], **Bogun Jang**[5], **Jimin Min**[2,4], **Joseph T. Roland**[2,4], **Qing Yang**[2,4,6], **William T. Fesmire**[2], **Sophie Camilleri-Broet**[7], **Lorenzo Ferri**[8], **Woo Ho Kim**[9], **Eunyoung Choi**[1,2,4], **James R. Goldenring**[1,2,3,4]

[1]Nashville VA Medical Center, Nashville, Tennessee

[2]Department of Surgery, Vanderbilt University School of Medicine, Nashville, Tennessee 37232

[3]Department of Cell and Developmental Biology, Vanderbilt University School of Medicine, Nashville, Tennessee 37232

[4]Epithelial Biology Center, Vanderbilt-Ingram Cancer Center, Vanderbilt University School of Medicine, Nashville, Tennessee 37232

[5]Department of Pathology, Jeju National University School of Medicine, Jeju, Korea

[6]Institute of Pathogen Biology, School of Basic Medical Sciences, Shandong University, Jinan 250012, China

[7]Department of Pathology, McGill University, Montreal, Canada

[8]Department of Surgery, McGill University, Montreal, Canada

[9]Department of Pathology, Seoul National University, Seoul, Korea

Abstract

Objectives: Intestinal type gastric adenocarcinoma arises in a field of pre-existing metaplasia. While biomarkers of cancer and metaplasia have been identified, the definition of dysplastic transition as a critical point in the evolution of cancer has remained obscure. We have evaluated Trop2 as a putative marker of the transition from metaplasia to dysplasia in the stomach.

Corresponding Author: James R. Goldenring, MD, PhD, AGAF, Epithelial Biology Center, Vanderbilt University School of Medicine, MRB IV 10435G, 2213 Garland Avenue, Nashville, TN 37232-2733, USA, Phone; 615-936-3726, Fax; 615-343-1591, jim.goldenring@vumc.org.

Author Contributions:

K. M. Riera: Designed and performed experiments, analyzed data, drafted manuscript.
B. Jang: Designed and performed experiments, analyzed data, revised manuscript.
J. Min: Designed and performed experiments, analyzed data, revised manuscript.
J. T. Roland: Designed and performed experiments, analyzed data, revised manuscript
Q. Yang: Performed experiments, analyzed data, revised manuscript.
W.T. Fesmire: Performed experiments, analyzed data
S. Camilleri-Broet: Designed experiments, revised manuscript.
L. Ferri: Designed experiments, revised manuscript.
W. Kim: Designed experiments, revised manuscript.
E. Choi: Designed experiments, analyzed data, revised manuscript.
J. R. Goldenring: Designed experiments, analyzed data, revised manuscript.

Disclosures: The authors have no conflicts of interest.

Design: Trop2 immunostaining was evaluated in multiple mouse models of metaplasia induction and progression. TROP2 expression in human samples was evaluated by immunostaining of tissue microarrays for metaplasia, dysplasia and gastric cancer. Dysplastic mouse organoids were evaluated *in vitro* following shRNA knockdown of Trop2 expression.

Results: In mouse models, no Trop2 was observed in the normal corpus and Trop2 was not induced in acute models of metaplasia induction with either L635 or DMP-777. In Mist1-Kras mice, Trop2 expression was not observed in metaplasia at one month after Kras induction, but was observed in dysplastic glands at 3–4 months after Kras induction. In human tissues, no Trop2 was observed in normal corpus mucosa or SPEM, but Trop2 expression was observed in incomplete intestinal metaplasia, with significantly less expression in complete intestinal metaplasia. Trop2 expression was observed in all dysplastic and 84% of gastric cancer lesions, although expression levels were variable. Dysplastic mouse organoids from Mist1-Kras mice expressed Trop2 strongly. Knockdown of Trop2 with shRNA markedly reduced organoid growth and budding behavior and induced the upregulation of apical villin expression.

Conclusion: Trop2 is upregulated in the transition to dysplasia in the stomach and promotes dysplastic cell behaviors.

Keywords

Tacstd2; dysplasia; metaplasia; gastric cancer; intestinal metaplasia; SPEM; CD44 variant 9

INTRODUCTION

Gastric cancer is the third leading cause of cancer death worldwide [1], with particularly high incidence rates in men and in Asian, Central/Eastern European, South American, and developing countries [2]. Intestinal-type gastric adenocarcinoma develops in the context of oxyntic atrophy and pre-existing metaplasia [3]. Spasmolytic Polypeptide (TFF2) Expressing Metaplasia (SPEM) represents the earliest metaplastic process associated with atrophy, which then evolves into intestinal metaplasia in the setting of chronic inflammation associated with chronic *Helicobacter pylori* infection, and ultimately predisposes to adenocarcinoma [4–6].

Recent studies have supported the concept that activation of the Ras/Raf/MEK/ERK (MAPK/ERK) pathway is important in gastric cancer progression [7,8], and chronic Kras activation in transgenic mice induces the full spectrum of SPEM and IM phenotypes in the gastric mucosa [9]. After 4 months of active Kras(G12D) expression in the stomach, focal areas of dysplastic cells can be identified, and dysplastic organoids with unique stem cells properties have been described recently [10]. Still, the transition points between metaplasia and dysplasia leading to adenocarcinoma remain elusive.

Trop2 is a transmembrane glycoprotein encoded by the tumor-associated signal transducer 2 (*tacstd2*) gene, and was first discovered as a trophoblast surface marker [11–14]. Trop2 is also known as trophoblast antigen 2, TACSTD2, membrane component 1 surface marker (M1S1), epithelial glycoprotein 1 (EGP-1), and gastrointestinal antigen 733–1 (GA733–1) [13,14]. Trop2 shares 50% sequence homology with EpCAM. Importantly, Trop2 has been

shown to promote tumor pathogenesis by activating the MAPK/ERK pathway [15–17], and has been identified as a possible therapeutic target in epithelia carcinomas [18]. Trop2 is upregulated in many epithelial human cancers, including breast, colon, non-small-cell lung, gastric, pancreatic, oral and esophageal squamous cell, cervical, ovarian, and gallbladder, and is associated with tumor aggressiveness, metastasis, and worse prognosis [14,16,19–34]. Inhibition of Trop2 with siRNA decreases tumor growth *in vitro* in low Trop2 expression colon and high Trop2 expression mammary cancer cells [27]. Treatment with sacituzumab govitecan (IMMU-132), an antibody drug conjugate SN-38 (topoisomerase I inhibitor) that is coupled to anti-Trop2 monoclonal antibody, had promising results for patients with refractory metastatic triple-negative breast cancer [35].

Previous studies have suggested that Trop2 overexpression overall predicts worse prognosis in human gastric cancer. In intestinal-type gastric cancer in an Austrian patient population, Trop2 overexpression was an independent prognostic marker for poor disease free survival (DFS) irrespective of lymph node involvement [29]. Additionally, for all gastric cancer types in this Austrian cohort, Trop2 overexpression was predictive for poor DFS and overall survival in lymph node positive patients. In Chinese populations, overexpression of Trop2 is similarly associated with poor prognosis, which worsens when co-expressed with amphiregulin [33,34]. However, the mechanistic role of Trop2 in gastric pre-neoplasia progression is not well understood, and Trop2 expression in other Asian or North American gastric cancer populations have not been investigated.

Trop2 is present in mouse stomach during fetal development and absent in adult mice except after epithelial injury [36]. In Immortomice stomach cell lineage lines, the *Tacstd2* gene was upregulated almost 60-fold in ImSPEM compared to ImChief cells in gene microarrays [37]. These results suggested that Trop2 expression may be up-regulated at transitions of lineage conversion. We have hypothesized that up-regulation of Trop2 may contribute to the lineage behavioral changes attendant with the transition from metaplasia to dysplasia. We have now investigated the patterns of Trop2 expression in mouse models of gastric pre-neoplasia as well as in human metaplasia, dysplasia and early cancer. In mice, Trop2 is not expressed in SPEM, but is highly upregulated in dysplastic glands in Mist1-Kras mice. In humans, Trop2 is absent in SPEM, but is upregulated in incomplete intestinal metaplasia and dysplasia. Trop2 knockdown in mouse dysplastic organoids leads to a decrease in organoid growth and amelioration of the dysplastic phenotype. The findings suggest that Trop2 is upregulated in the transition from metaplasia to gastric dysplasia.

METHODS

All authors had access to the study data and reviewed and approved the final manuscript.

Mouse metaplasia models

Mist1-Kras mouse stomachs.—We studied Trop2 staining in Mist1-Cre^{ERT2};LSL-K-Ras(G12D) (Mist1-Kras) mice, which express the constitutively active form of Kras (Kras(G12D)) in gastric chief cells when treated with tamoxifen. All samples were from archival blocks from our previous investigations, specifically, eight week old Mist1-Kras mice were treated with 5 mg subcutaneous tamoxifen for 3 doses to induce expression of

Kras(G12D) in chief cells [9]. Mist1-Kras mice developed SPEM, IM, and invasive/dysplastic lesions at 1, 3, and 4 months post-tamoxifen treatment, respectively [9]. Control Mist1-Kras mice were sacrificed 4 months after corn oil administration. Stomachs from all mice were fixed in 4% paraformaldehyde (PFA), and paraffin embedded with standard tissue processing. All samples were in triplicate.

Oxyntic atrophy models of metaplasia.—Archival paraffin blocks of stomachs from mice were used to evaluate Trop2 expression in established mouse models of SPEM induction [38]. For acute models of oxyntic atrophy, samples were obtained from mice treated with L635 for 0 and 3 days (SPEM with inflammation) or DMP-777 for 0 and 14 days (SPEM without inflammation). To investigate chronic SPEM induction model with inflammation, samples were obtained from mice after infection with *Heliobacter felis* for 6 or 12 months. All samples were performed in triplicate. All mouse stomachs were fixed in 4% PFA, paraffin embedded, and prepared for histology. Samples were stained with immunofluorescence for Ki67, Trop2, and CD44v9.

Trop2 knockdown Meta4 organoids

We have recently reported on the characterization of dysplastic organoids derived from Mist1-Kras mice, designated Meta4 [10]. Meta4 mouse organoids were harvested from Mist1-Kras mice 4 months after induction with tamoxifen [10]. Meta4 organoids, as previously described, were plated in 30 μl of Matrigel (Sigma) per well in a 48-well tissue culture plate and incubated in Mouse Intesticult media (StemCell Technologies) with penicillin/streptomycin with refeeding every 3 days.

To investigate Trop2 as a functional driver of pre-neoplastic progression, Meta4 organoids were transfected using lentivirus to knock down Trop2. Three shRNA vectors, designated 1, 2 and 3 (see Supplemental Table 3), as well as a scrambled control shRNA were utilized to prepare lentivirus in HEK cells as previously described [39]. Vectors were transfected into HEK cells for 48 hours and media was collected with packaged lentivirus, and the virus was concentrated. Meta4 organoids were split 2 days prior to infection. Two wells of organoids per viral group were washed with PBS and spun at 300g for 5 min. TrypLE (Thermo Fisher) was added to the organoids and the organoids were incubated for 3 minutes at 37°C and then washed with DMEM/F12 (Thermo Fisher) with 10% FBS and spun down at 300g for 5 minutes. Pellets were directly resuspended onto a 48-well plate with 350 μl of Mouse Intesticult media with penicillin/streptomycin, mycozap, Y27632, 0.64 μl of 5 mg/ml polybrene and 50 μl of virus per well. Plates were spinoculated at 32°C at 600g for 1 hour and incubated overnight without Matrigel. Organoids were split, washed, and spun down twice with 10 ml of DMEM-F12 with 10% FBS and then plated in 30 μl of Matrigel per well in a 48-well plate and fed with 300 μl of Mouse IntestiCult media. Organoids were fed every 3–4 days and split when appropriate. Transfected organoids were selected for Trop2 knockdown constructs with puromycin 2 μg/ml added to media, cultured for 30 days, and then harvested.

The whole well images of Meta4 and the three shRNA Trop2 knockdown organoid lines were captured at day 0, 6, 9 and 14 in 3D cultures using the JuLI™ Stage (NanoEntek). Two

to four wells of each organoid line were captured and the experiments were repeated twice. For quantitation of budding rates, a total 20 to 300 organoids were considered from each image taken at day 14 and the number of organoids which formed budding structures were manually counted. For measurement of organoid diameters, images taken at day 14 were used and a total of 50 organoids were considered from each experiment for each organoid line. The diameters were manually measured for each organoid. Statistical differences were analyzed by Student's t-test compared with the control Meta4 line.

The organoids were harvested by fixing with 4% PFA for 30 minutes at room temperature, washed, resuspended in HistoGel, and paraffin embedded by standard tissue processing. Paraffin sections of organoids were stained for H&E and processed for immunofluorescence staining with antibodies for Trop2, Villin and Hoechst for nuclear staining.

Western blot analysis

Proteins were extracted from control Meta4 organoids as well as three shRNA Trop2 knockdown lines using M-PER lysis buffer (Thermo Fisher) with protease and phosphatase inhibitor cocktails. The Direct Detect IR spectrometer (Millipore) was used to measure protein concentration. For protein separation, 7 μg of total protein were loaded onto a Mini-Protean TGX Precast Gel (Bio-Rad). The separate proteins were transferred to a nitrocellulose membrane (Bio-Rad) for protein detection. The membranes were incubated with the Odyssey blocking solution (LI-COR Biosciences) for 1 hour at room temperature for blocking and incubated overnight at 4°C with Trop2 anti-goat (R&D systems AF1122, 1:2,000) and β-Actin anti-mouse (Sigma A5316, AC-74, 1:5,000) diluted in the Odyssey blocking solution supplemented with 0.2% Tween-20. After washing with TBS-T three times, the membranes were incubated with IRDye 800CW donkey anti-goat (LI-COR Biosciences 926–32214, 1:10,000) and IRDye 680LT donkey anti-mouse secondary antibody (LI-COR Biosciences 926–68022, 1:10,000) for 1 hour at room temperature. The membranes were washed with TBS-T three times and imaged with an Odyssey imaging system (LI-COR Biociences).

Immunofluorescence staining for mouse gastric tissue and Meta4 organoids

Paraffin embedded slide sections were deparaffinized with Histoclear, hydrated and antigen retrieved with 1x pH6 citrate buffer (stock solution: Dako Target Retrieval Solution 10x) using a pressure cooker for 15 minutes. Slides were cooled, washed, and then protein blocked (Dako Protein Block Serum-Free solution) for 1.5 hours at room temperature. Primary antibodies (see Supplemental Table 2) were incubated overnight at 4°C in Dako Antibody Diluent with Background Reducing Components. Slides were washed three times and then species-specific secondary antibodies (see Supplemental Table 2) were incubated with Cy2, Cy3 and Cy5 secondary antibodies (1:500) for 1 hour at room temperature in Dako Antibody Diluent followed by another three washes. Nuclear staining was performed with DAPI or Hoechst with exact concentrations noted in figure legends. Slides were washed three times and coverslipped with Prolong Gold (Thermo Fischer Scientific).

Image analysis for mouse gastric tissue and Meta4 organoids

All bright field and immunofluorescent slides were scanned using a Lieca SCN400 or a Leica Versa 200 imaging system in the Digital Histology Shared Resource (DHSR). Immunofluorescence staining of mouse stomach and Meta4 organoids was imaged using a Nikon A1R confocal microscope. All phase contrast images of organoids were obtained using the JuLI™ Stage imaging microscope (Nanoentek). Images were analyzed in Adobe Photoshop CC (version 19.1.3).

Korean human gastric dysplasia and gastric cancer arrays.

One tissue array was assembled from dysplastic adenomas at Seoul National University Hospital (SNUH). Two separate human gastric cancer array sets were constructed with specimens obtained from SNUH and Jeju National University Hosptial (JNUH) in Korea. The Korean Cancer arrays contained de-identified patient demographic, staging, histologic characteristics and survival data. In total, 19 tissue arrays containing normal antral and fundic glands, intestinal metaplasia (IM), dysplastic adenomas and early or advanced gastric cancers were generated from SNUH samples. In a second set, 8 tissue arrays containing normal antral and fundic glands, IM and early gastric cancers were constructed from JNUH samples.

Fluorescence staining in Korean Dysplasia Array from SNUH

One tissue array slide with 30 cores total (23 adenomas and 7 cores with no dysplasia as controls) was stained for immunofluorescence. Using multiplex imaging, slides were processed using staining protocol described above until after protein block, at which point the array was wet mounted with a Hoechst 1:1000 solution with for imaging on Cytell microscope with GE CellDive software for digital H&E. The array slide was de-coverslipped in PBS and primary antibodies for human Trop2, TFF3 and CD44v9 were incubated overnight at 4°C following staining protocol as described above. Species-specific secondary antibodies were incubated for 1 hour at room temperature for Cy2 and Cy3. The slide underwent nuclear staining with Hoechst 1:1000 wet mount and was imaged with the Cytell microscope for whole slide fluorescent scanning. The array was imaged and individual channels from individual cores were reassembled in Adobe Photoshop. Digital H&E images were analyzed individually by Dr. Jang, who annotated specifically dysplastic areas within the tissue.

Fluorescence staining in Korean Early Gastric Cancer Array from JNUH

Eight array slides with 192 cores were stained with immunofluorescence. Using multiplex imaging, slides were processed using the staining protocol above until after protein block, at which point arrays were wet mount with 50/50 glycerin/PBS and 1:5000 DAPI for imaging on a Leica Versa 200 to create digital H&E with a whole slide fluorescent scanning platform. Slides were decoverslipped in PBS and primary antibodies for TFF3, Trop2, CD44v9, and PCNA were incubated overnight at 4°C following staining protocol as described above. Species-specific secondary antibodies were incubated for 1 hour at room temperature for Cy2, Cy3, Cy5, and Alexa 750. Slides were wet mounted with glycerin/PBS/Hoechst solution and imaged on the Leica Versa 200 imager for

immunofluorescence. Three cores were lost during the staining process. Staining index in cancer regions for Trop2, CD44v9 and TFF3 images was stratified as follows: 0 = no staining, 1 = staining in up to 25% of cells, 2 = in 25–50% of cells, 3 = staining in greater than 50% of cells.

Immunohistochemical staining in Korean Gastric Cancer Array from SNUH

Immunohistochemistry was conducted on a 4-μm tissue array section using a BOND-MAX automated immunostainer and a Bond Polymer Refine Detection kit (Leica Microsystems, Wetzlar, Germany) according to the manufacturer's instructions. The primary antibody used was anti-Trop2 (R&D Systems, Minneapolis, MN, USA; 1:800). The expression of Trop2 was determined by examining the cell membrane and the intensity and percentage of cells expressing Trop2 were evaluated. Histology index (H index) was calculated by multiplying the intensity score (0 = negative; 1 = weak; 2 = moderate; 3 = strong) and percentage of positive cells (range = 0–100), to obtain a score range from 0 to 300.

Dysplastic Adenomas from McGill University, Canada

Sections from four deidentified cases of dysplastic adenomas were stained for CD44v9 and Trop2 along with DAPI as above. Sections were imaged on the Lecia Versa 200 using a 20X objective.

Statistical analysis

Student's t-test was used to calculate statistical differences between control Meta4 line and the three shRNA Trop2 knockdown organoid lines. For analysis Trop2 immunostaining in early gastric cancer arrays, H indexes were compared by ANOVA with post hoc comparison of significant means with Tukey's test (Prism). For analysis of survival based on H indexes for Trop2 immunostaining, Kaplan-Meier method was used with the PASW 18.0 statistical software program (IBM SPSS Statistics, Chicago, IL, USA).

RESULTS

Trop2 expression in mouse models of metaplasia and dysplasia

We have recently reported that Mist1-Kras mice develop the full range of metaplastic changes from SPEM to IM and then dysplasia over a four month period after tamoxifen induced expression of dominant-active Kras(G12D) in Mist1-expressing chief cells in the gastric corpus [9]. We therefore sought to examine the expression of Trop2 during the initiation and progression of metaplasia in Mist1-Kras mice. We first examined Trop2 expression in the normal mouse stomach. While we observed strong plasma membrane staining in the mouse forestomach, no staining was detected in the corpus or antral epithelial cells (Figure 1A). At one month after Kras(G12D) induction where the mucosa is predominantly replaced with pyloric-type SPEM glands, prominent upregulation of CD44v9 and hyperproliferation were observed (Figure 1A). However, no staining for Trop2 was present in any sample. At three months after active Kras induction, a point when intestinal metaplasia is observed [9], scattered Trop2 positive cells were observed in 23% of glands (Figure 1A and B). By four months after induction, when intestinal metaplasia predominates and scattered dysplastic glands were observed, prominent expression of basolateral Trop2

was found throughout the metaplastic mucosa in over 50% of corpus glands (Figure 1A and B). In general, we observed that cells showing strong staining for Trop2 exhibited reduced staining for CD44v9, a marker of SPEM. In addition, the cells that strongly expressed basolateral CD44v9 at the bases of glands showed little or no staining for Trop2. The Trop2-expressing lineages appeared in association with and luminal to the zone of proliferation.

To evaluate whether Trop2 was up-regulated in other models of metaplasia development in the mouse stomach, we evaluated staining in sections from mice treated with DMP-777 or L635 to induce acute parietal cell loss and SPEM, as well as in sections from 6-month and 12-month *H. felis*-infected mice (Supplemental Figure 1). While we observed prominent staining of Trop2 in the forestomach, no basolateral Trop2 staining was observed in SPEM induced by acute oxyntic atrophy. Similarly, SPEM in 6 month or 12 month *H. felis*-infected mice also did not express Trop2 (Figure 2). These results suggested that SPEM was not significantly associated with Trop2 expression.

TROP2 expression in human patient stomach tissues.

We sought to evaluate the relevance of our results in the mouse models in human patient tissues. We first performed immunohistochemical staining to evaluate TROP2 expression in the normal human stomach and pathological tissues in a set of tissue arrays from patients at Seoul National University Hospital (Supplemental Table 1). No significant specific staining for TROP2 was observed in normal human corpus and only occasional basolateral TROP2 staining was observed in cells at the bases or at the surface of individual antral glands (Figure 2A). We next evaluated expression of TROP2 in intestinal metaplasias and gastric cancers. Quantitation of immunohistochemical staining demonstrated significantly higher labeling indices for TROP2 in incomplete intestinal metaplasia compared to either normal stomach samples or complete intestinal metaplasia (Figure 2A). Figure 2B demonstrates the presence of basolateral Trop2 staining in regions of incomplete intestinal metaplasia, but not in complete intestinal metaplasia.

We also evaluated the expression of TROP2 in gastric adenomas and gastric cancers. While tubular adenomas demonstrated mild elevations in the levels of TROP2 staining, gastric cancers expressed significantly higher levels of TROP2. Intestinal-type, diffuse and mixed cancers all showed similar levels of TROP2 staining (Figure 2A and Supplemental Figure 2). We also examined whether TROP2 protein expression was prognostic for survival in patients with gastric cancer. Figure 2C demonstrates that TROP2 expression was not predictive of survival in any of the case groups. We additionally evaluated whether a complete absence of TROP2 had any influence on survival, and again no significant effect was observed (data not shown).

Since our initial findings demonstrated an up-regulation of TROP2 in incomplete intestinal metaplasia, we next examined in greater detail the topology of TROP2 expression in early gastric cancer arrays comparing TROP2 expression to expression of TFF3 as an intestinal metaplasia marker and CD44v9 as a marker of SPEM. In the early gastric cancer samples, a number of cores contained regions with metaplasias, intramucosal dysplasia and invasive cancer. Figure 3A shows one such region where submucosal invasive gastric cancer was strongly positive for membrane-associated TROP2. Within the mucosa regions of SPEM

were positive for CD44v9, but negative for TROP2. In contrast, we were able to identify regions of complete or incomplete intestinal metaplasia which were negative for CD44v9. Glands with complete intestinal metaplasia showed strong TFF3 expression, but no TROP2 (Figure 3A, arrowheads). In contrast, regions with incomplete intestinal metaplasia showed smaller granules and more diffuse TFF3 expression associated with strong membrane staining for TROP2.

To compare the expression of TROP2 with CD44v9, a strong marker of SPEM, and TFF3, a marker of intestinal metaplasia, we compared staining patterns for these proteins in 166 cores containing early gastric cancers. Figure 3B demonstrates that while greater than 80% of cancers showed prominent staining for TROP2, a similar percentage of tumors showed an absence of very weak staining for CD44v9. Similarly, TFF3 was relatively less prominent in the early gastric cancers. Overall staining indices for TROP2 were significantly higher in the cancers than staining for either CD44v9 or TFF3 (Figure 3C).

We further evaluated staining for TROP2 in a tissue array assembled from specimens of intramucosal dysplasia. 100% of the 23 tissue cores with dysplasia showed basolateral TROP2 staining. None of the cores without dysplasia showed any TROP2 staining. Figure 4A demonstrates the typical pattern of dysplasia expressing TROP2 with an adjacent region of SPEM that expressed CD44v9, but not TROP2. No detectable CD44v9 staining was observed in 22/23 dysplasia samples. Only one out of the 23 cases showed CD44v9 expression retained in TROP2-positive dysplastic cells (Figure 4B). Many samples showed TROP2 positive dysplasia completely replacing the mucosal lineages (Figure 4C). Since there has been some controversy over whether the carcinogenic cascade is the same among western and Asian patients, we also examined staining for TROP2 and CD44v9 in for cases of dysplasia identified at McGill University in non-Asian patients. Supplemental Figure 3 demonstrates staining in two of the patients with strong TROP2 staining in dysplasia adjacent to CD44v9 positive, TROP2 negative SPEM. All these results support the concept that TROP2 expression increases in the context of incomplete intestinal metaplasia and dysplasia.

Trop2 expression in mouse Meta4 dysplastic organoids

We have recently developed dysplastic organoids isolated from Mist1-Kras mice 4 months after the induction of Kras(G12D) expression with tamoxifen [10]. These organoids display a number of dysplastic properties, including aggressive budding formation, multilayered growth and growth in soft agar. We stained the Meta4 organoids for Trop2 and found high levels of expression in the basolateral membranes of Meta4 cells (Figure 5B). To evaluate the impact of Trop2 on dysplastic organoid behavior, we infected Meta4 organoids with 3 different lentiviral shRNA constructs targeting Trop2. The lentiviral shRNAs induced varying levels of knockdown of Trop2 expression by both western blot and Trop2 immunostaining (Figure 5A and 5B). To evaluate the effects of shRNA knockdown of Trop2 on organoids growth and behavior, we cultured control Meta4 organoids and the 3 Trop2 knockdown organoid lines for 2 weeks in Matrigel (Figure 5C). Remarkably, the Trop2 knockdown lines exhibited markedly slower growth with significantly smaller organoids diameters in the Trop2 shRNA-expressing lines (Figure 5D). In addition, we observed a

change in the morphology of the organoids with Trop2 knockdown with assumption of more spherical structures that generally showed single layers of cells in contrast with the budding and multilayered phenotype in control Meta4 organoids (Figure 5E). We have previously shown that Meta4 organoids treated with a MEK inhibitor showed reduced organoid growth and budding and up-regulation of villin at the apical membranes of organoid cells, consistent with the differentiation of cells toward an absorptive enterocyte phenotype [10]. We therefore examined the pattern of villin expression in Meta4 organoids and in two of the shRNA-expressing lines. While Meta4 cells showed no detectable expression of villin at their apical membranes, the Trop2 shRNA-expressing organoids showed strong apical villin expression (Figure 5F) in 26/31 organoids examined (84%). These results indicate that down-regulation of Trop2 expression can lead to induction of a more benign differentiated phenotype in Meta4 organoids.

DISCUSSION

Since intestinal type gastric cancer arises within a field of pre-existing metaplasia, recurrent surveillance endoscopy is the standard of care for those with extensive metaplasia in the stomach, even after *H. pylori* eradication. At the heart of any surveillance program for gastric cancer is a focus on identifying early cancer or intramucosal dysplastic lesions that are amenable to curative endoscopic or surgical resection. Since it is assumed that dysplastic lesions arise from within regions of metaplasia, the identification of markers within metaplasia that indicate risk for transition from metaplasia to dysplasia has been a major focus over the past years [40]. It is known that incomplete intestinal metaplasia is a major increased risk factor, especially compared with complete intestinal metaplasia [41]. But patients often have a mixture of complete and incomplete intestinal metaplasia and SPEM lesions that are often not clearly delineated in biopsies with hematoxylin and eosin stains. Previous studies have suggested that expression of CD44v9 is characteristic of SPEM lineages, with declining expression in intestinal metaplasia and cancer [42–44]. The present investigations demonstrate that expression of TROP2 develops strongly in association with incomplete intestinal metaplasia and is highly characteristic of dysplastic lesions and early gastric cancers.

An understanding of the process of gastric carcinogenesis has been hampered by a lack of mouse models that recapitulate the patterns for progressive development of metaplasia, dysplasia and adenocarcinoma. We have demonstrated that Mist1-Kras mice develop SPEM with 1 month after induction of Kras(G12D) expression in chief cells [9]. By 3 months after induction, Mist1-Kras mice develop TFF3 and Muc2-expressing intestinal metaplasia and at 4 months after induction dysplastic glands are observed [9]. At present the Mist1-Kras mouse represents the only mouse model that demonstrates the full spectrum of progression of metaplastic lineages from SPEM to intestinal metaplasia to dysplasia. The glands in Mist1-Kras mice at 4 months post-induction are dominated with intestinal metaplasia lineages expressing TFF3 [9], but they do not contain Paneth cells or CCK-expressing enteroendocrine cells. Thus, these glands may display lineage patterning more characteristic of incomplete intestinal metaplasia. These findings in the mouse model would therefore be consistent with our observation of up-regulation of Trop2 in human incomplete intestinal metaplasia.

We have recently reported the development of Meta4 organoid lines from Mist1-Kras mice 4 months after induction that display many features of dysplastic behavior, including piling of cells, growth in soft agar and the ability to engraft in the stomach wall [10]. These Meta4 organoids strongly express Trop2. Importantly, the knockdown of Trop2 in these dysplastic organoids not only reduced organoid growth, but also changed organoid morphology with adoption of a single layer spheroid pattern, which is more characteristic of benign organoids. Furthermore, as in the case of MEK inhibitor treatment [10], knockdown of Trop2 expression in Meta4 organoids led to marked up-regulation of apical villin expression, characteristic of the assumption of a well-differentiated intestinal absorptive cell. Trop2 expression was not observed in SPEM lesions and was upregulated in intestinal metaplasia and dysplastic glands in Mist1-Kras mice at 3 to 4 months after induction. Thus, these studies in mouse models support the concept that Trop2 expression rises at a critical point at the junction between metaplasia and dysplasia and may be responsible in part for the adoption of more aggressive and invasive behaviors associated with dysplasia. Previous investigations have linked Trop2 expression with increases in phospho-ERK [15], so upregulation of Trop2 may be acting as a promoter of Ras activation.

A number of previous studies have noted the up-regulation of Trop2 in gastric cancers [29,33,34]. These prominent increases have led to targeting of Trop2 with specific antibodies with bifunctional properties to induce targeted tumor destruction [45]. It is similarly possible that such strategies could be used to detect and even treat dysplastic lesions that may be present within patients with extensive metaplasia. We have recently suggested that treatment of rodents with extensive metaplasia with MEK inhibitors can arrest metaplasia and allow repopulation of the gastric mucosa with normal lineages [9,46]. It therefore seems possible that inhibition of MEK and targeting of Trop2-expressing lineages may provide novel therapeutic approaches to reducing risk for developing cancer in patients with extensive incomplete intestinal metaplasia and dysplasia in the stomach.

In conclusion, the present studies have shed light on Trop2 as a critical biomarker that is upregulated in the transition from metaplasia to dysplasia. Thus, expression of Trop2 within regions of intestinal metaplasia may be an indicator of increased risk. Prospective trials will be required to examine this association in patients with multiple screening biopsies to assess the utility of this marker as a prognostic indicator of gastric cancer risk.

Supplementary Material

Refer to Web version on PubMed Central for supplementary material.

ACKNOWLEDGEMENTS

These studies were supported by grants from a Department of Veterans Affairs Merit Review Award IBX000930, DOD CA160479, NIH R01 DK071590 and R01 DK101332 and a Cancer UK Grand Challenge Award 29075 (to J.R.G), DOD W81XWH-17-1-0257, and AACR 17-20-41-CHOI and pilot funding from NIH P30 DK058404 (to E.C). K.R. was supported by NCI T32 CA106183. Q.Y. was supported by the China Scholarship Council (Grant No. 201706225033). This work was supported by core resources of the Vanderbilt Digestive Disease Center (NIH P30 DK058404) and Vanderbilt Ingram Cancer Center (P30 CA068485) with imaging in the Vanderbilt Digital Histology Shared supported by a VA Shared Instrumentation grant (1IS1BX003097).

REFERENCES

1. Ferlay J, Soerjomataram I, Dikshit R, et al. Cancer incidence and mortality worldwide: sources, methods and major patterns in GLOBOCAN 2012. Int J Cancer 2015; 136: E359–386. [PubMed: 25220842]
2. Bray F, Ferlay J, Soerjomataram I, et al. Global cancer statistics 2018: GLOBOCAN estimates of incidence and mortality worldwide for 36 cancers in 185 countries. CA: a cancer journal for clinicians 2018; 68: 394–424. [PubMed: 30207593]
3. Correa P, Piazuelo MB. The gastric precancerous cascade. Journal of digestive diseases 2012; 13: 2–9. [PubMed: 22188910]
4. Lennerz JKM, Kim S, Oates EL, et al. The transcription factor MIST1 is a novel human gastric chief cell marker whose expression is lost in metaplasia, dysplasia and carcinoma. Amer J Pathol 2010; 177: 1514–1533. [PubMed: 20709804]
5. Schmidt PH, Lee JR, Joshi V, et al. Identification of a metaplastic cell lineage associated with human gastric adenocarcinoma. LabInvest 1999; 79: 639–646.
6. Goldenring JR, Nam KT, Wang TC, et al. Spasmolytic polypeptide-expressing metaplasia and intestinal metaplasia: time for reevaluation of metaplasias and the origins of gastric cancer. Gastroenterology 2010; 138: 2207–2210. [PubMed: 20450866]
7. Cancer Genome Atlas Research N. Comprehensive molecular characterization of gastric adenocarcinoma. Nature 2014; 513: 202–209. [PubMed: 25079317]
8. Tan IB, Ivanova T, Lim KH, et al. Intrinsic subtypes of gastric cancer, based on gene expression pattern, predict survival and respond differently to chemotherapy. Gastroenterology 2011; 141: 476–485, 485 e471–411. [PubMed: 21684283]
9. Choi E, Hendley AM, Bailey JM, et al. Expression of Activated Ras in Gastric Chief Cells of Mice Leads to the Full Spectrum of Metaplastic Lineage Transitions. Gastroenterology 2016; 150: 918–930. [PubMed: 26677984]
10. Min J, Vega PN, Engevik AC, et al. Heterogeneity and dynamics of active Kras-induced dysplastic lineages from mouse corpus stomach. Nature communications 2019; 10: 5549.
11. Ripani E, Sacchetti A, Corda D, et al. Human Trop-2 is a tumor-associated calcium signal transducer. Int J Cancer 1998; 76: 671–676. [PubMed: 9610724]
12. Lipinski M, Parks DR, Rouse RV, et al. Human trophoblast cell-surface antigens defined by monoclonal antibodies. Proc Natl Acad Sci U S A 1981; 78: 5147–5150. [PubMed: 7029529]
13. McDougall AR, Tolcos M, Hooper SB, et al. Trop2: from development to disease. Developmental dynamics : an official publication of the American Association of Anatomists 2015; 244: 99–109. [PubMed: 25523132]
14. Shvartsur A, Bonavida B. Trop2 and its overexpression in cancers: regulation and clinical/therapeutic implications. Genes & cancer 2015; 6: 84–105. [PubMed: 26000093]
15. Cubas R, Zhang S, Li M, et al. Trop2 expression contributes to tumor pathogenesis by activating the ERK MAPK pathway. Molecular cancer 2010; 9: 253. [PubMed: 20858281]
16. Cai H, Jing C, Chang X, et al. Mutational landscape of gastric cancer and clinical application of genomic profiling based on target next-generation sequencing. Journal of translational medicine 2019; 17: 189. [PubMed: 31164161]
17. Agoston AT, Odze RD. Evidence that gastric pit dysplasia-like atypia is a neoplastic precursor lesion. Human pathology 2014; 45: 446–455. [PubMed: 24529328]
18. Cubas R, Li M, Chen C, et al. Trop2: a possible therapeutic target for late stage epithelial carcinomas. Biochim Biophys Acta 2009; 1796: 309–314. [PubMed: 19683559]
19. Nakashima K, Shimada H, Ochiai T, et al. Serological identification of TROP2 by recombinant cDNA expression cloning using sera of patients with esophageal squamous cell carcinoma. Int J Cancer 2004; 112: 1029–1035. [PubMed: 15386348]
20. Liu T, Liu Y, Bao X, et al. Overexpression of TROP2 predicts poor prognosis of patients with cervical cancer and promotes the proliferation and invasion of cervical cancer cells by regulating ERK signaling pathway. PLoS ONE 2013; 8: e75864. [PubMed: 24086649]

21. Tang G, Tang Q, Jia L, et al. High expression of TROP2 is correlated with poor prognosis of oral squamous cell carcinoma. Pathology, research and practice 2018; 214: 1606–1612.
22. Ohmachi T, Tanaka F, Mimori K, et al. Clinical significance of TROP2 expression in colorectal cancer. Clin Cancer Res 2006; 12: 3057–3063. [PubMed: 16707602]
23. Chen MB, Wu HF, Zhan Y, et al. Prognostic value of TROP2 expression in patients with gallbladder cancer. Tumour biology : the journal of the International Society for Oncodevelopmental Biology and Medicine 2014; 35: 11565–11569. [PubMed: 25135430]
24. Fong D, Moser P, Krammel C, et al. High expression of TROP2 correlates with poor prognosis in pancreatic cancer. Br J Cancer 2008; 99: 1290–1295. [PubMed: 18813308]
25. Fong D, Spizzo G, Gostner JM, et al. TROP2: a novel prognostic marker in squamous cell carcinoma of the oral cavity. Mod Pathol 2008; 21: 186–191. [PubMed: 18084248]
26. Zhao P, Yu HZ, Cai JH. Clinical investigation of TROP-2 as an independent biomarker and potential therapeutic target in colon cancer. Mol Med Rep 2015; 12: 4364–4369. [PubMed: 26059528]
27. Trerotola M, Cantanelli P, Guerra E, et al. Upregulation of Trop-2 quantitatively stimulates human cancer growth. Oncogene 2013; 32: 222–233. [PubMed: 22349828]
28. Xu N, Zhang Z, Zhu J, et al. Overexpression of trophoblast cell surface antigen 2 as an independent marker for a poor prognosis and as a potential therapeutic target in epithelial ovarian carcinoma. Int J Exp Pathol 2016; 97: 150–158. [PubMed: 27127000]
29. Muhlmann G, Spizzo G, Gostner J, et al. TROP2 expression as prognostic marker for gastric carcinoma. J Clin Pathol 2009; 62: 152–158. [PubMed: 18930986]
30. Inamura K, Yokouchi Y, Kobayashi M, et al. Association of tumor TROP2 expression with prognosis varies among lung cancer subtypes. Oncotarget 2017; 8: 28725–28735. [PubMed: 28404926]
31. Chen K, Yang D, Li X, et al. Mutational landscape of gastric adenocarcinoma in Chinese: implications for prognosis and therapy. Proc Natl Acad Sci U S A 2015; 112: 1107–1112. [PubMed: 25583476]
32. Aihara E, Matthis AL, Karns RA, et al. Epithelial Regeneration After Gastric Ulceration Causes Prolonged Cell Type Alterations. Cell Molec Gastroent Hepatol 2016; 2: 625–647.
33. Zhao W, Ding G, Wen J, et al. Correlation between Trop2 and amphiregulin coexpression and overall survival in gastric cancer. Cancer medicine 2017; 6: 994–1001. [PubMed: 28256068]
34. Zhao W, Zhu H, Zhang S, et al. Trop2 is overexpressed in gastric cancer and predicts poor prognosis. Oncotarget 2016; 7: 6136–6145. [PubMed: 26716416]
35. Bardia A, Mayer IA, Vahdat LT, et al. Sacituzumab Govitecan-hziy in Refractory Metastatic Triple-Negative Breast Cancer. N Engl J Med 2019; 380: 741–751. [PubMed: 30786188]
36. Fernandez Vallone V, Leprovots M, Strollo S, et al. Trop2 marks transient gastric fetal epithelium and adult regenerating cells after epithelial damage. Development 2016; 143: 1452–1463. [PubMed: 26989172]
37. Weis VG, Petersen CP, Mills JC, et al. Establishment of novel in vitro mouse chief cell and SPEM cultures identifies MAL2 as a marker of metaplasia in the stomach. Amer J Physiol: GI & Liver Physiol 2014; 307: G777–792.
38. Weis VG, Sousa JF, LaFleur BJ, et al. Heterogeneity in mouse SPEM lineages identifies markers of metaplastic progression. Gut 2013; 62: 1270–1279. [PubMed: 22773549]
39. Schlegel C, Lapierre LA, Weis VG, et al. Reversible deficits in apical transporter trafficking associated with deficiency in diacylglycerol acyltransferase. Traffic 2018; 19: 879–892. [PubMed: 30095213]
40. Eriksson NK, Karkkainen PA, Farkkila MA, et al. Prevalence and distribution of gastric intestinal metaplasia and its subtypes. Dig Liver Dis 2008; 40: 355–360. [PubMed: 18291729]
41. Gonzalez CA, Sanz-Anquela JM, Companioni O, et al. Incomplete type of intestinal metaplasia has the highest risk to progress to gastric cancer: results of the Spanish follow-up multicenter study. J Gastroenterol Hepatol 2016; 31: 953–958. [PubMed: 26630310]
42. Meyer AR, Engevik AC, Willet SG, et al. Cystine/Glutamate Antiporter (xCT) Is Required for Chief Cell Plasticity After Gastric Injury. Cell Mol Gastroenterol Hepatol 2019.

43. Bertaux-Skeirik N, Wunderlich M, Teal E, et al. CD44 variant isoform 9 emerges in response to injury and contributes to the regeneration of the gastric epithelium. J Pathol 2017; 242: 463–475. [PubMed: 28497484]

44. Go SI, Ko GH, Lee WS, et al. CD44 Variant 9 Serves as a Poor Prognostic Marker in Early Gastric Cancer, But Not in Advanced Gastric Cancer. Cancer Res Treat 2016; 48: 142–152. [PubMed: 25779358]

45. Zhao W, Jia L, Zhang M, et al. The killing effect of novel bi-specific Trop2/PD-L1 CAR-T cell targeted gastric cancer. American journal of cancer research 2019; 9: 1846–1856. [PubMed: 31497363]

46. Yang Q, Yasuda T, Choi E, et al. MEK Inhibitor Reverses Metaplasia and Allows Re-Emergence of Normal Lineages in Helicobacter pylori-Infected Gerbils. Gastroenterology 2019; 156: 577–581 e574. [PubMed: 30391471]

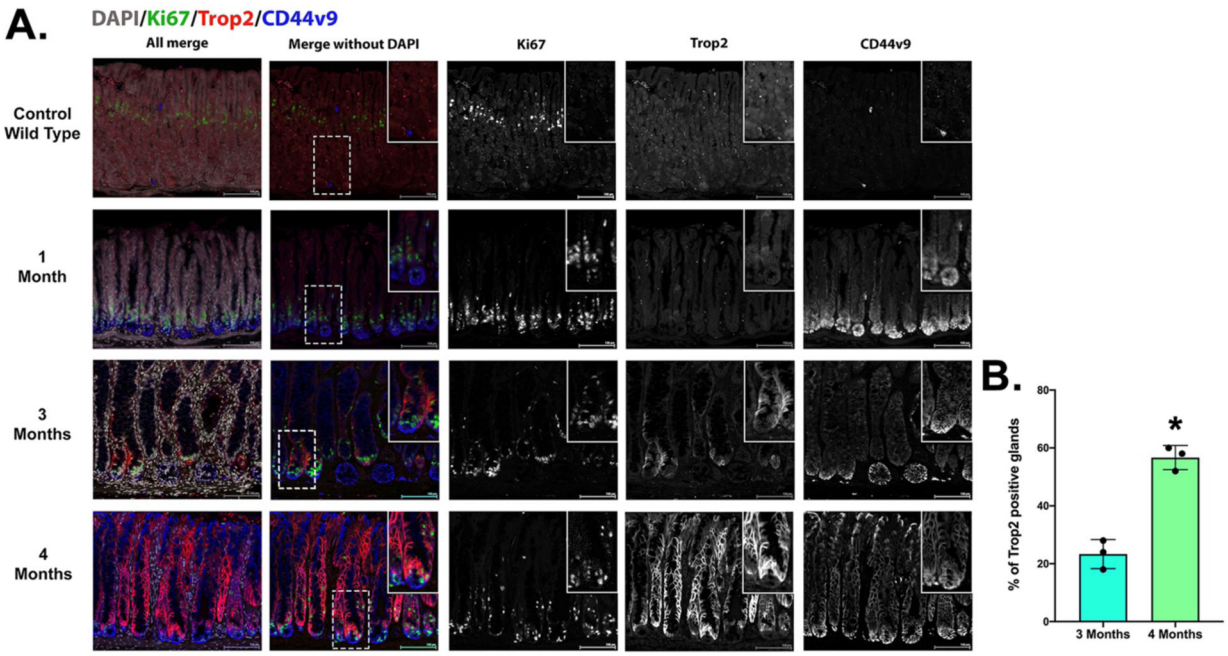

Figure 1: Trop2 expression is up-regulated 3 to 4 months after induction of Kras(G12D) expression in Mist1-Kras mice.

A. Sections of mouse stomach from uninduced Mist1-Kras mice (Control Wild type) and mice 1, 3 and 4 months after Kras(G12D) induction with tamoxifen treatment were stained for CD44v9 (blue), Ki67 (green) and Trop2 (red) along with nuclear staining with DAPI (greyscale). Scale bar = 100 μm. B. The percentage of glands with Trop2 positive cells was quantified (50 glands per mouse) in the corpus of Mist1-Kras mice 3 or 4 months after tamoxifen induction (n=3 mice). No glands were positive in mice (n=3) at 1 month after induction. Data are shown as mean±S.D. *<0.05 by Mann-Whitney U.

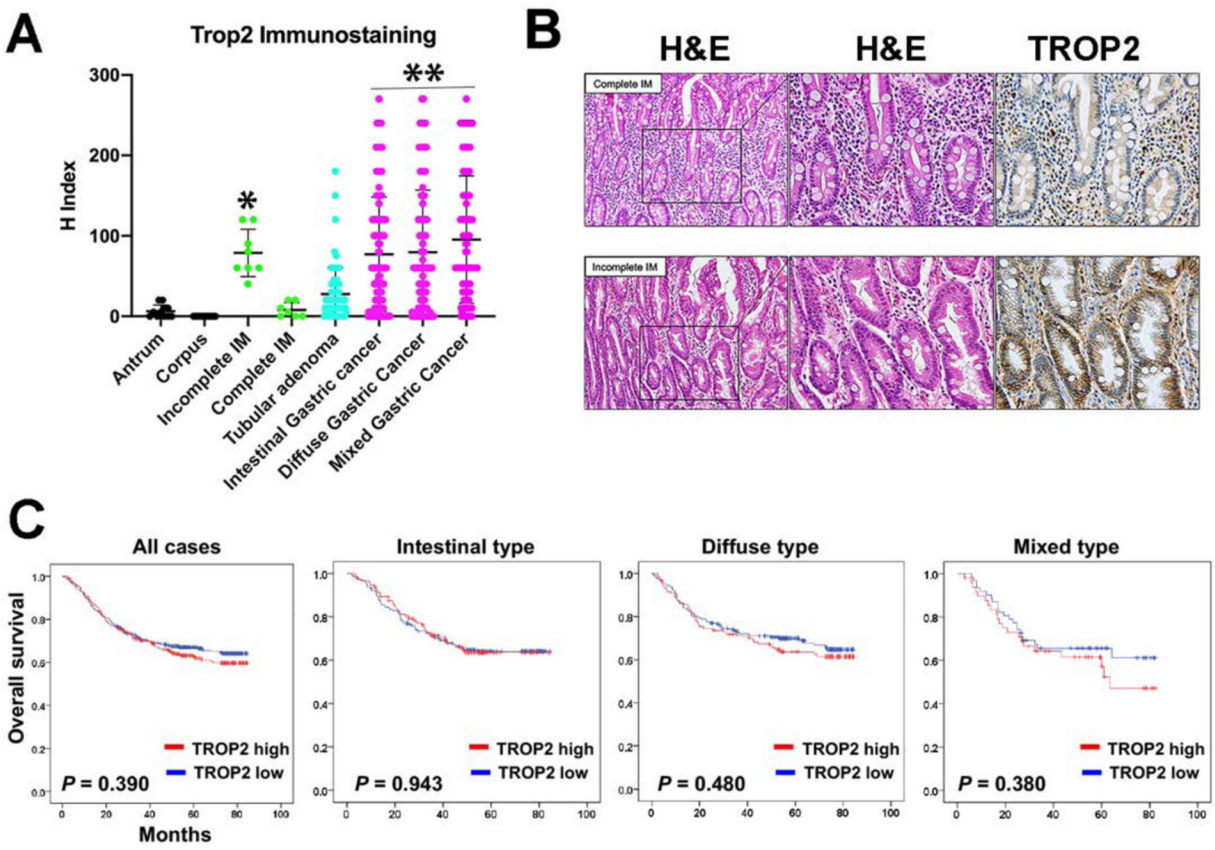

Figure 2: TROP2 expression is higher in incomplete intestinal metaplasia (IM), adenoma and cancer.

A. Tissue arrays containing normal, metaplastic, adenomatous and cancer lesions were stained with antibodies against TROP2 with immunohistochemistry: antrum (n = 11), corpus (n = 13), incomplete IM (n = 8), complete IM (n = 7), tubular adenoma (n = 71), intestinal type gastric cancer (n = 289), diffuse type gastric cancer (n = 334), mixed type gastric cancer (n = 111). Staining was quantified for each core by histology index (H Index). Data are shown for mean±SD. Significance by Tukey's test was *p<0.01 versus normal or complete intestinal metaplasia; **p<0.001 versus all non-cancer samples. B. Examples of TROP2 immunostaining in complete and incomplete IM. Serial sections were stained with hematoxylin and eosin (H&E) and TROP2 immunohistochemistry. Higher magnification of the delineated region is shown for hematoxylin and eosin and TROP2 immunohistochemistry (far right). Basolateral TROP2 staining was prominently present in incomplete IM, but was absent in complete IM. C. Kaplan-Meyer survival curves for gastric cancers based on TROP2 staining.

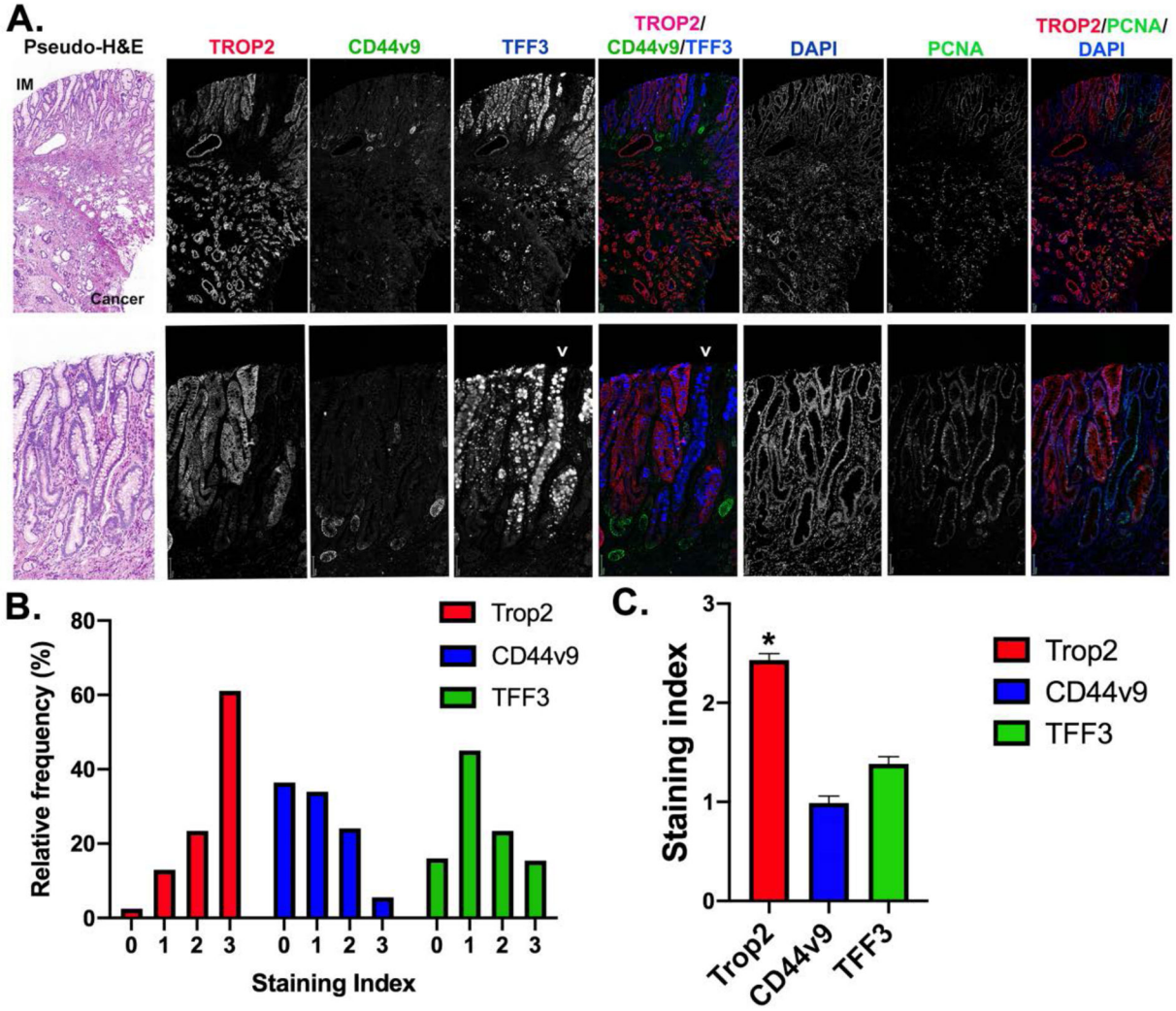

Figure 3: Expression of TROP2 in a cancer, dysplastic lineages and IM.

A. representative core from tissue microarrays of early gastric cancers. The slides were stained for TROP2 (red), CD44v9 (green) and TFF3 (blue) as well as PCNA (green) and DAPI (blue). Single channel images are shown in grayscale for all, with triple composite overlays as noted. Higher magnification images are shown in the second row. A pseudo-H&E image is shown at the left. Arrowhead marks the position of a gland with intestinal metaplasia and strong TFF3 staining goblet cells without TROP2 expression, while the TFF3 expressing glands to the left have small granules and strong TROP2 staining. Bars = 100 μm. B and C. Staining indexes for TROP2, CD44v9 and TFF3 were calculated for 166 early gastric cancer cores represented on the arrays. B. Data are represented showing the distribution of staining index for each of the three markers. C. Date are represented as mean ±SEM for each of the markers. The staining for TROP2 in the early cancers was significantly higher than for either TROP2 or CD44v9 (*$p<0.001$).

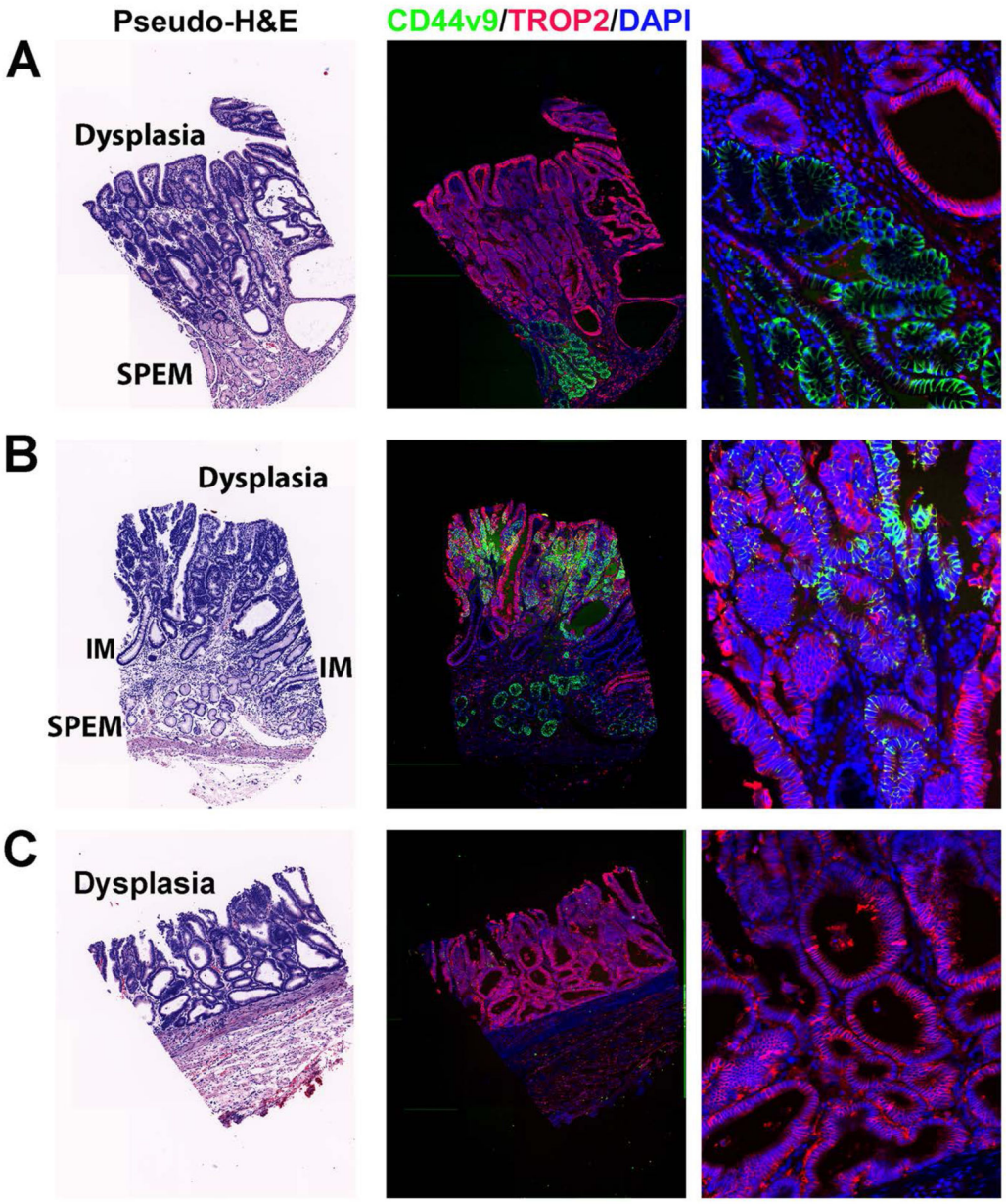

Figure 4: Expression of TROP2 in human metaplasia and dysplasia.

Representative staining of cores from tissue microarrays of samples of intramucosal dysplasia. Slides were stained for TROP2 (red), CD44v9 (green) and DAPI (blue). A higher magnification image is shown at the right. A pseudo-H&E stain image is shown at the left. Regions of dysplasia, SPEM and IM are noted in the H&E. A. An example of TROP2-positive dysplasia arising above CD44v9-positive SPEM. B. A rare case of TROP2-positive dysplasia observed in only 1 out of 60 cores that also showed strong positivity for CD44v9. C. An example of intramucosal dysplasia that is positive for only TROP2.

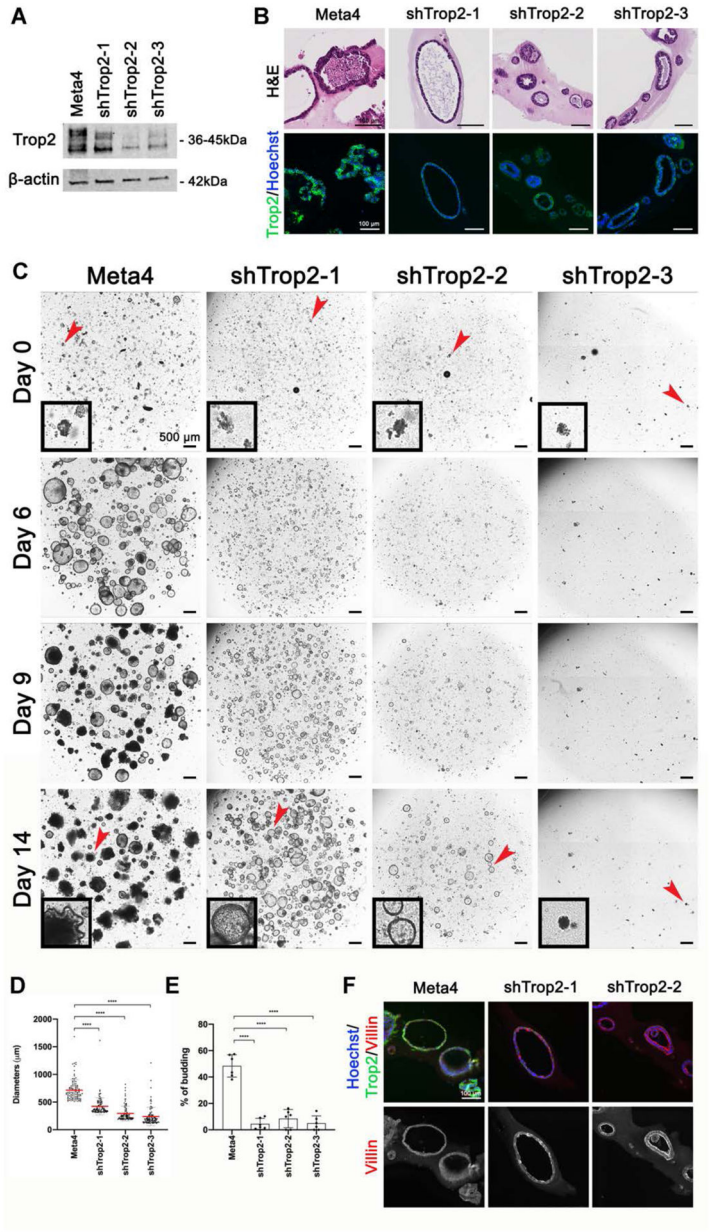

Figure 5: Knockdown of Trop2 in dysplastic organoids decreases growth and normalizes morphology.

A. Western blot for Trop2 demonstrates strong expression of Trop2 in Meta4 organoids, with decreased expression in organoids lines stably infected with 3 different shRNA lentiviral vectors (shTrop2–1, shTrop2–2 and shTrop2–3). B. Representative H&E stains and immunofluorescence staining for Trop2 (green) and Hoechst nuclear stain (blue) in Meta4 organoids, shTrop2–1, shTrop2–2 and shTrop2–3. Bar = 100 μm. Note the growth of knockdown organoids as single layer spheres compared with the complex multilayered structures in Meta4 organoids. C. Phase contrast imaging of live Meta4 and shRNA Trop2 knockdown organoids growing in Matrigel culture for 0, 6, 9 and 14 days. Note the reduced growth and budding formation in the Trop2 knockdown organoids, shTrop2–1, shTrop2–2 and shTrop2–3. Black box insets display a representative organoid at Day 0 and 14. Red

arrowheads indicate enlarged area. Bar = 500 μm. D. Diameters (μm) of Meta4 (n=100), shTrop2–1 (n=100), shTrop2–2 (n=100) and shTrop-3 (n=77) measured after 14 days in 3D cultures. Data are shown for mean ± SD. The p values were calculated using Mann-Whitney test. ****p<0.0001. E. Quantitation of the average budding rate in Meta4 organoids and the 3 shRNA Trop2 knockdown organoid lines, shTrop2–1, shTrop2–2 and shTrop2–3, after 14 days in 3D cultures. Data are shown for mean ± SD. The p values were calculated using unpaired t-test. ****p<0.0001. F. Immunofluorescence staining for Trop2 (green), Villin (red) and Hoechst nuclear stain (blue) in Meta4, shTrop2–1 and shTrop2–2 organoids. Bar = 100 μm.